SYMPOSIUM PROCEEDINGS

RP-34-94 Swan, David, Dickinson Arikara and Prabhu
Fuel Cell Dynamics in Transit Applications

Volume 1, Sessions 1A-2D
Poster Sessions

THE 12TH INTERNATIONAL ELECTRIC VEHICLE SYMPOSIUM (EVS-12)

and Electric Vehicle Exposition

Presented by

Electric Vehicle Association of the Americas (EVAA)

Sponsored by

Edison Electric Institute
Electric Power Research Institute
Ford Motor Company
General Motors Corporation
U.S. Department of Energy

EVS-12

**Paper not available at time of printing.*

FUEL CELL DYNAMICS IN TRANSIT APPLICATIONS

David H. Swan, Blake Dickinson
Murali Arikara, Manohar Prabhu
Institute of Transportation Studies
University of California, Davis, 95616

Abstract

This paper presents experimental data on the dynamic response of a proton exchange membrane (PEM) fuel cell system. By varying the electrical load to the USABC Dynamic Stress Test (DST) standard the fuel cell underwent a load pattern similar to what electric vehicle batteries are now subjected. The fuel cell system used was a Ballard Power Systems' 35 cell stack with 232 cm^2 of active electrode area per cell employing Nafion-117 electrolyte membrane. The primary objective of the experiments was to determine the influence dynamic load and cathode air compression would have on the fuel cell efficiency. Intelligent air compressor control was found to be critical to maximize net efficiency. This paper represents part of a series of experiments that are now being conducted at UC Davis to establish dynamic response characteristics of fuel cells and fuel cell hybrids for transportation applications.

Introduction

Transit buses are a favored early application for fuel cell use in transportation[1]. Using a fuel cell power system can provide the long range of a conventional transit bus with rapid refueling. Emissions can be zero if hydrogen is the boarded fuel or near zero if methanol and a reformer are used. The electric propulsion system will be similar that in a battery powered bus.

However, there is a fundamental difference between a battery and a fuel cell in how each is operated. For a storage battery no control or operational scheme is required to draw the power from the battery. The propulsion system simply draws current as necessary or returns it under regenerative braking conditions. The operation of a fuel cell is more like a conventional engine. When the driver demands power the fuel cell system must respond by going from an idle to a power state. Regenerative braking power cannot be stored by the fuel cell. As a result the propulsion system and the fuel cell power system must be controlled as cooperative systems.

A fuel cell power plant is a complex group of systems that must dynamically operate to provide power to the bus propulsion system, as can be seen in Figure 1. To meet the varying driving load conditions the fuel cell power plant must frequently go from an idle state to full power and return to idle. The rate of these changes and duration at each power level depends on the fuel cell size, driving profile and use in a hybrid configuration (along with a storage battery).

[1]Currently two fuel cell powered buses are being tested. Ballard Power Systems and the US Department of Energy.

A fuel cell is an energy conversion device and needs the necessary reactants (hydrogen and air) to be supplied to its electrodes to create the power demanded. If hydrogen is boarded on the vehicle the fuel side is relatively easy, the fuel cell simply draws fuel as necessary. The air supply side is substantially more difficult. Under dynamic conditions the quantity of air and its pressure are a function of the electrical load applied on the fuel cell. The response time, flow rate and operating pressure of the air compressor and its parasitic power demand plays a critical role in the operation of the fuel cell and its net efficiency. For background information, the reader is referred to a previous characterization of the same fuel cell stack under steady-state operating conditions (1). Previous investigation of similar dynamic characteristics can be found in Oliveira et al (2), Dickinson et al (3) and a description of a fuel cell powered bus can be found in Howard and Greenhill (4).

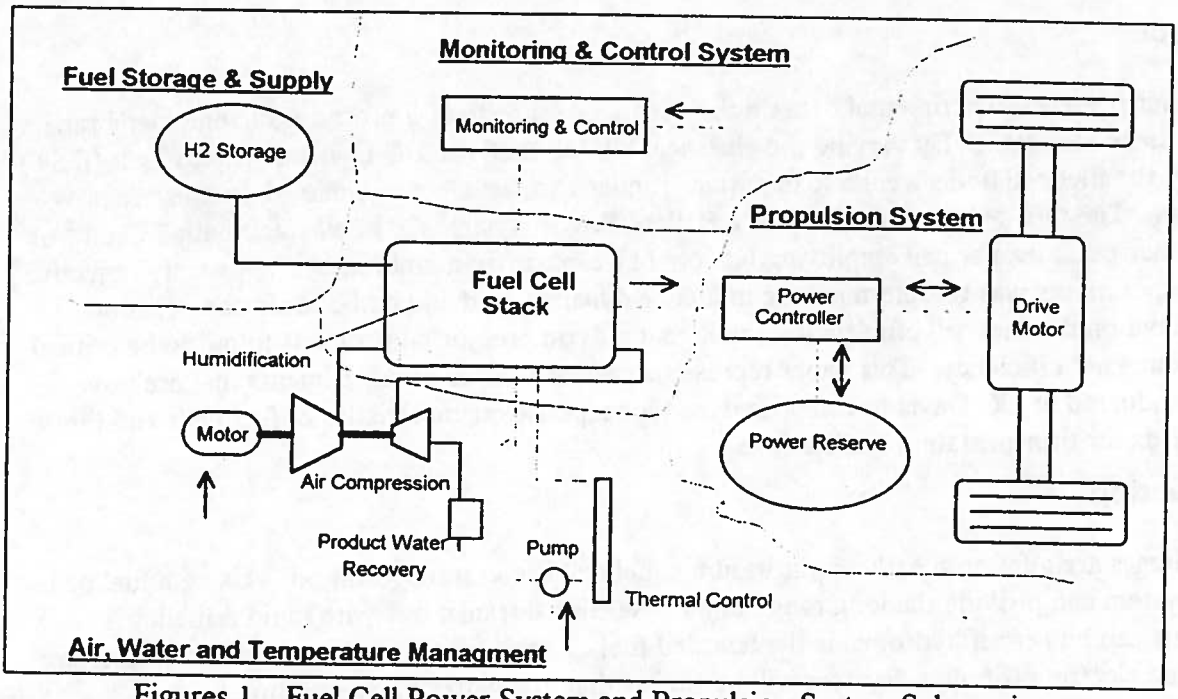

Figures 1. Fuel Cell Power System and Propulsion System Schematic

Fuel Cell Operating Principle

All energy-producing oxidation reactions are fundamentally the same and involve the release of chemical energy through the transfer of electrons. During combustion of hydrogen and oxygen there is an immediate transfer of electrons, heat is released and water is formed. In a fuel cell the hydrogen and oxygen do not immediately come together but are separated by an electrolyte. First the electrons are separated from the hydrogen molecule by a catalyst (oxidation) creating a hydrogen ion (no electrons). The ion then passes through the electrolyte to the oxygen side. The electrons cannot pass through the electrolyte and are forced to take an external electrical circuit which leads to the oxygen side. The electrons can provide useful work as they pass through the external circuit. When the electrons reach the oxygen side they combine with the hydrogen ion and oxygen creating water. By forcing the electrons to take an external path, a low temperature direct energy conversion is achieved as shown in Figure 2.

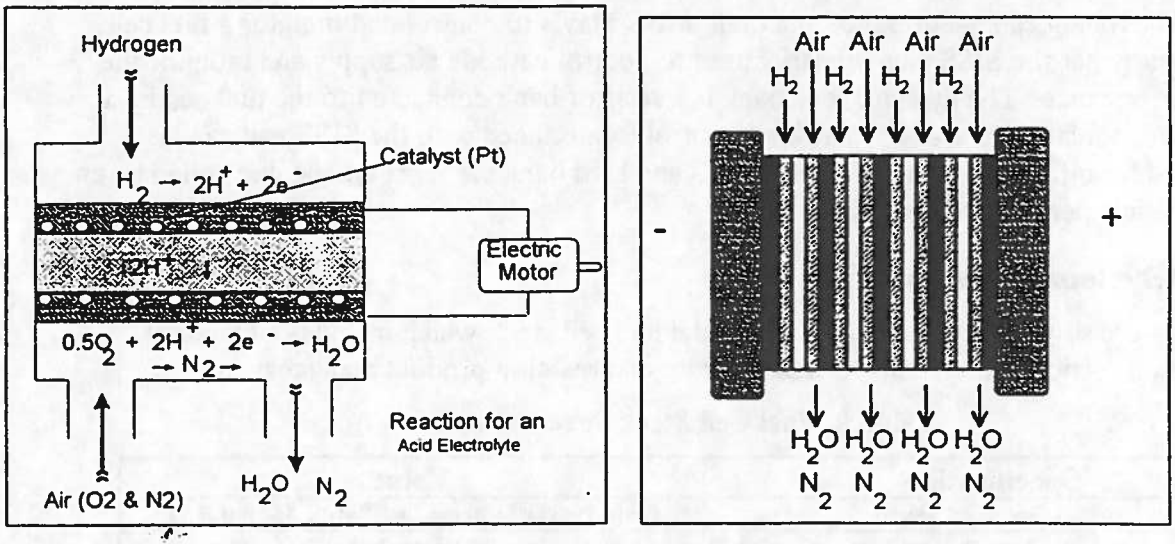

Figures 2. and 3. Fuel Cell Operation and Stack Schematic

Like a storage battery, when the fuel cell is under electrical load the voltage falls with maximum power generally being produced between 0.5 and 0.6 volts per cell. The voltage drop as a function of current is due to internal resistance (electronic and ionic), electrode kinetics (particularly on the air electrode), reactant gas flow limitations and product water flooding of reaction sites. To make a useful voltage, multiple cells are connected in electrical series, referred to as a stack as shown in Figure 3. Manifolds deliver reactant gases to the reaction sites. The fuel cell stack and all necessary auxiliaries are referred to as a fuel cell system.

The fuel cell stack design must allow for heat exchange and humidification of incoming reactant gases, thermal management, product water management, exhaust gases, and electrical management.

Experimental Setup

The experimental setup consisted of the fuel cell stack, a stack instrumentation and support system (SISS) and a dynamic load bank as shown in Figure 4.

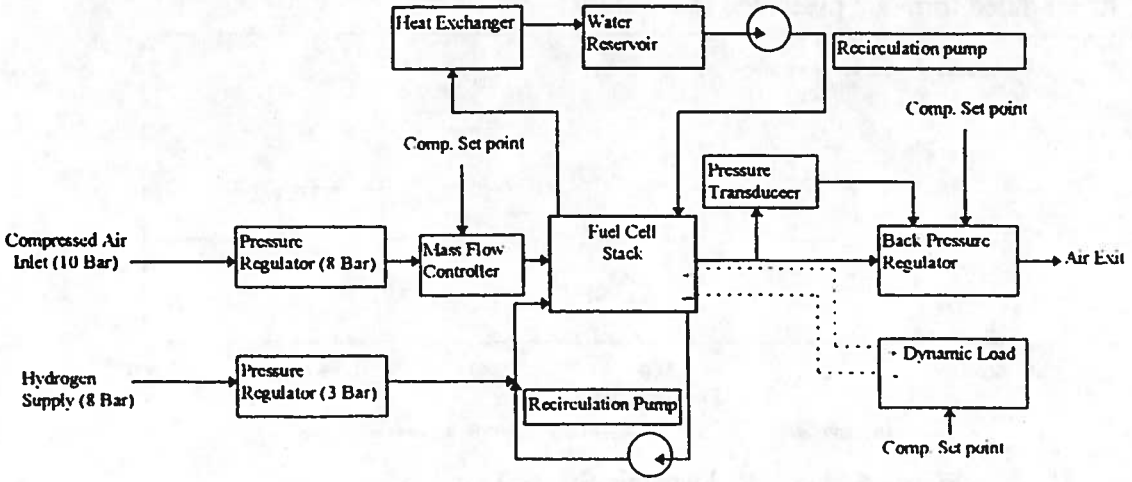

Figure 4. Schematic of Experimental Setup

The SISS is a rolling cabinet designed and built at UC Davis to control and monitor a fuel cell stack. In this paper the SISS was primarily used to control cathode air supply and monitor the fuel cell performance. The dynamic load bank is a resistor bank connected to the fuel cell by a pulse-width-modulated controller. The load control is interfaced with the SISS and can be programmed for different load cycles. The SISS and load bank were set up and controlled by an IBM-compatible personal computer.

Fuel Cell System Description

Given below are some of the specifications for the fuel cell stack which includes an integral humidification section and systems for temperature and reaction product management.

Table 1. Fuel Cell Stack Specifications

Specification	Value
Manufacturer / Model	Ballard Power Systems / PGS-103 [Serial # 115]
Electrolyte	Nafion-117
Number of Active Cells	35
Active Area/Cell	232 cm2
Total Active Area	8120 cm2
Active Cell Thickness	0.5 cm
# of Cooling Cells	19
Active Plate Thickness	0.5 cm
# of Humidification Cells	14
Fuel Cell Stack Dimensions LxWxH	45.5 x 25 x 25cm*
Fuel Cell Stack Volume	28.4 liters*

*Includes active stack with humidification section, cooling cells and end plates (box volume)

Dynamic Stress Test

The fuel cell stack was loaded according to the Dynamic Stress Test (DST) developed by the United States Advanced Battery Consortium (USABC) to evaluate advanced batteries under dynamic conditions (5). The USABCs test cycles set a standard by which alternative power system technologies can also be compared to one another. However, since the fuel cell cannot accept the regenerative portions of the DST cycle these were ignored. The profile of the six-minute DST and its modified form are presented in Figure 5.

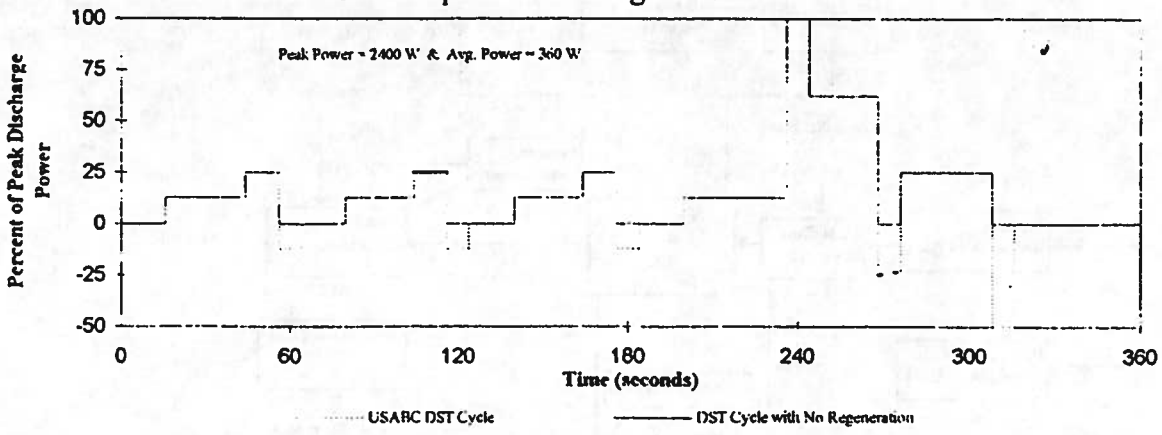

Figure 5. USABC Dynamic Stress Test

The peak power of 2400 Watts represents a rate of discharge that can be achieved by the stack under all dynamic conditions. Transitions between power discharge levels were achieved within one second, as specified by the USABC for the DST cycle.

Experimental Procedure

For the performance measurements of the fuel cell stack, five different cases were considered. The five cases were selected as a first approximation to determine the influence of dynamic operation on the fuel cell stack and the energy needs for cathode air compression. The first case was under steady state electrical load conditions. The following 4 cases were all under dynamic (DST) electrical load. The dynamic load cases explored the effect of varying the cathode air stoichiometry and the cathode exit back pressure. The following text and table describes each of the 5 cases.

Case 1: Steady State Electrical Load. The fuel cell was operated under steady state conditions by selecting fixed electrical loads (0 to 2400 Watts in 300 Watt increments) at a fixed cathode air stoichiometry (S=2)and cathode exit air temperature.

Case 2: Dynamic Electrical Load, Constant Cathode Air Flow Rate, Constant Cathode Exit Air Back Pressure. The fuel cell was operated under dynamic load with a fixed cathode air flow rate of 116.6 standard liters per minute (SLM). (This flow rate corresponds to a stoichiometry of 2 at a current of 100 amps.) This case represents the simplest air compressor control scheme: a fixed displacement air compressor operating at a constant pressure and flow rate.

Case 3: Dynamic Electrical Load, Constant Cathode Air Flow Rate, Varying Cathode Exit Air Back Pressure. The fuel cell was operated under dynamic load with a fixed cathode air flow rate of 116.6 SLM (same as case 2) and a variable cathode exit back pressure. The back pressure was varied from a minimum of 2 bar to a maximum of 3 bar. The minimum of 2 bar was due to experimental apparatus limitations. This case represents the second most simple air compressor control scheme: a fixed displacement air compressor operating into a variable pressure.

Case 4: Dynamic Electrical Load, Varying Cathode Air Flow Rate, Constant Cathode Exit Air Back Pressure. The fuel cell was operated under dynamic load with a varying cathode air flow rate corresponding to a stoichiometry of 2, with the cathode exit back pressure held to 3 bar. This case represents the air compressor control scheme where the flow rate is varied depending on electrical load but the cathode air pressure is maintained.

Case 5: Dynamic Electrical Load, Varying Cathode Air Flow Rate, Varying Cathode Exit Air Back Pressure. The fuel cell was operated under dynamic load with a varying cathode air flow rate corresponding to a stoichiometry of 2 and a variable cathode exit back pressure. The back pressure was varied from a minimum of 1.4 bar to a maximum of 3 bar. The wider pressure swing compared to case 3 was possible due to the lower cathode air flow rates. This case represents the most complicated air compressor control scheme: variable flow rate and air pressure.

It should be noted that for all 4 dynamic cases the effective compressor was turned off during zero power periods of the DST.

Results

By utilizing Equation (1) the stack conversion efficiency (Stack Efficiency) for the steady state case was calculated. A major consumer of the fuel cell power is the cathode air compressor (6). To achieve a suitable power density the cathode air is compressed to increase the partial pressure of oxygen and thus increase the fuel cell electrode kinetics. The conducted experiments monitored cathode inlet flow rate and pressure. For this paper the compressor energy required to supply the fuel cell was calculated from the adiabatic compression equation (7). Adiabatic compression was chosen as a close approximation of real compression (some where between adiabatic and isothermal). No allowance was made for pressure recovery at the cathode air exit.

Stack Efficiency: $$\frac{\int V(t)\times I(t)\,dt}{\int I(t)\,dt}\times\frac{100\%}{35\times 1.25}\ (\%) \qquad (1)$$

Compression: $$P_c = C_p\times T_1\times\left[\left(\frac{P_2}{P_1}\right)^{\frac{(k-1)}{k}}-1\right]\times SLM\times\frac{1\,min}{60sec}\times\frac{1}{\bar{v}}\times M\ (Watts) \qquad (2)$$

Net Efficiency: $$\frac{\int V(t)\times I(t)\,dt-\int P_c(t)\,dt}{\int I(t)\,dt}\times\frac{100\%}{35\times 1.25}\ (\%) \qquad (3)$$

Where C_p *Specific Heat (Air 1.004 J/(g K),*
T_1 *Compressor Inlet Air Temperature (K),*
P_1 *Compressor Inlet Air Pressure (bar),*
P_2 *Compressor Outlet Air Pressure (bar),*
v *Specific Volume on a Molar Basis (22.4 L/Mole),*
M *Molecular Mass (28.97 g/mole for Air).*
V *Stack Voltage (volts),*
I *Stack Current (amps),*
k *Specific Heat Ratio,*
35 Cells in the Stack
1.25 Theoretical Cell Voltage Based on Enthalpy of Formation (Lower) (volts),

Each of the dynamic cases were averaged over three consecutive DST cycles. By integrating the power and current over the three cycles the total Watt hours and amp hours were found. The fuel cell stack conversion efficiency was then determined utilizing Equation (1). The net energy as described in this paper is the difference of the measured cycle energy output and the calculated energy required for an adiabatic compressor to supply air to the fuel cell stack. Using measured cathode pressure and flow rates the dynamic power requirements for the adiabatic compressor were calculated and integrated over the DST cycles. Equation (2) shows the power required for an adiabatic compressor as a function of flow rate and pressure. By subtracting the compressor energy from the fuel cell stack energy the net energy and resultant efficiency were calculated. During zero power periods in the DST the effective compressor was turned off and hence the energy of compression was zero for those periods.

The resultant stack and net efficiencies for the 5 different cases are presented in the following bar chart. Case 1 (steady state case) represents the efficiency of the fuel cell stack at a constant power of 360 Watts. The other 4 cases represent values as the result of integrating the performance over the DST.

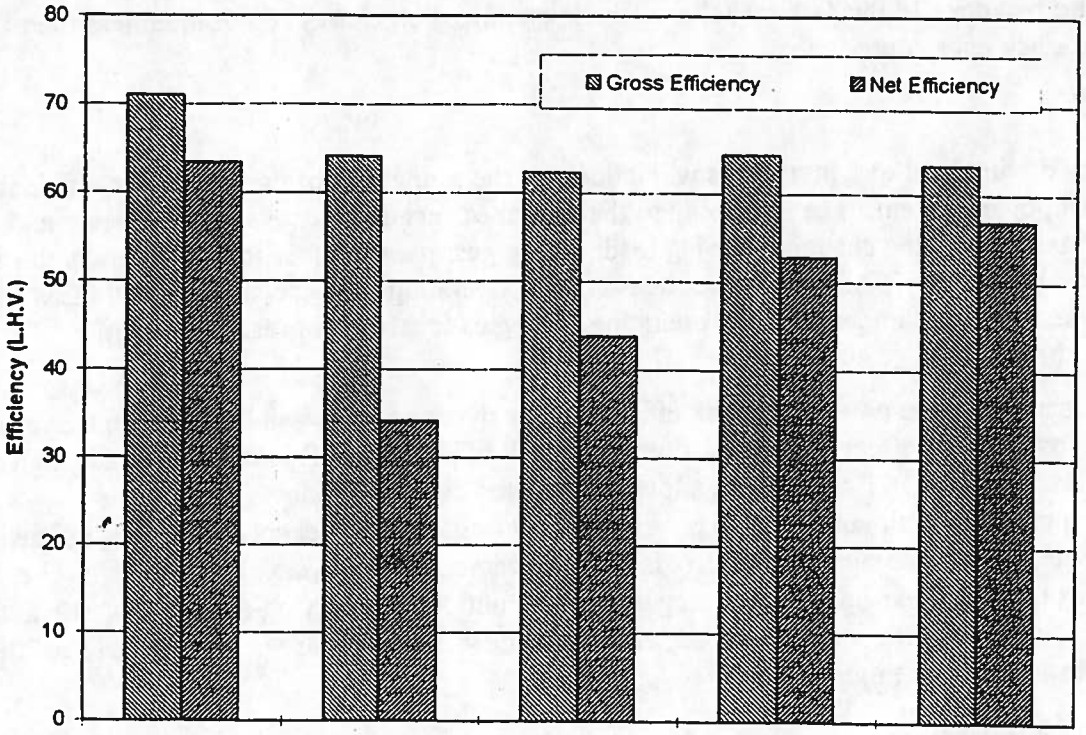

Condition	Case 1	Case 2	Case 3	Case 4	Case 5
Description	Steady State	Dynamic-Constant Compressor Inputs	Dynamic-Vary Back Pressure	Dynamic-Vary Air Flow Rate	Dynamic-Vary Air Flow and Back Pressure
Electrical Load	Steady State 360 W	DST*	DST*	DST*	DST*
Air Supply	S = 2	116 SLM	116 SLM	S = 2	S = 2
Air Pressure	3 Bar	3 Bar	2 to 3 Bar	3 Bar	1.4 to 3 Bar

* Average Cycle Power = 360 Watts. Cathode Air Exit Temperature = 60 °C

Figure 6. Fuel Cell Efficiency as Function of Air Compressor Control

As expected the steady state case provided the highest stack and net efficiency. Compared to the steady state case all the dynamic cases have a lower stack efficiency. This is predominately the result of the high power part of the DST resulting in a lower average weighted voltage over the cycle (due to the increase in the IR drop). In case 2, the stoichiometry was varied throughout the entire cycle (the stoichiometry was high for the entire cycle except at maximum power where it equals 2) and the pressure maintained at 3 Bar, as a result the compression energy required is high and the net efficiency is low. In case 3 the pressure was varied as a function of the load. Lower pressure of air was used for the lower load regions. The lower pressure resulted in a slight reduction in the stack efficiency but the decrease in compression energy resulted in a high net efficiency. In case 4 the pressure was held to 3 Bar and the stoichiometry held to 2. The constant stoichiometry resulted in a varying cathode flow rate through the stack. The stack efficiency increased to approximately the same level as case 2 indicating that the excessive air used in that case provided no extra benefit. However the reduced flow rate resulted in a lower compression energy resulting in a higher net efficiency. The last case where the flow rate and pressure were varied as a function of load resulted in a slightly lower stack efficiency but the

highest net efficiency. In this last case the adiabatic compression energy represented less than 10% of the stack energy produced.

Summary

The varying driving load of a transit bus will influences the sizing, performance and net efficiency of a fuel cell power system. The air supply to the described fuel cell must vary in flow rate and pressure to respond to the changing driving load. The largest parasitic loss to the system is the air compressor. Using the USABC dynamic stress test the operating efficiency of a 35 cell PEM fuel cell stack was measured under different operating strategies for the compressed air supply. To summarize the findings

1. For the same average power the stack efficiency of a dynamic cycle will be less than that at a steady power. This affect is predominately the result of increased IR losses during the high power levels of the DST resulting in a lower integrated cycle efficiency.
2. Air compression for air supply can have a significant impact on a fuel cell system net efficiency and power. The air compressor control is critical over a dynamic cycle. By comparing the results of four different operating strategies it was found that by varying the air flow rate and pressure there was little impact on stack efficiency and a large increase in net efficiency of the fuel cell system. See Figure 6.

Acknowledgments

The authors wish to thank Ballard Power Systems and California Department of Transportation (New Technologies Division) for the support they have provided for the Fuel Cell Laboratory at the Institute of Transportation Studies, Davis. We also wish to thank the University of California Transportation Center for financially supporting the graduate students involved in this project.

References

1. D.H. Swan, B.E. Dickinson, and M.P. Arikara, "Proton Exchange Membrane Fuel Cell Characterization for Electric Vehicle Applications," SAE Paper 940296, presented at the 1994 SAE International Congress, Detroit, Michigan (February 28 - March 3).
2. Julio C.T. Oliveira, A. Anantaraman and W.A. Adams. "Performance Evaluation of a H_2/Air PEM-FC System under Variable Load." 1992 Fuel Cell Seminar: Fuel Cell Program and Extracts, pp. 451-454 (1992).
3. B.E. Dickinson, T. Lalk, and D. G. Hervey. "Characterization of a Fuel Cell/Battery Hybrid System for Electric Vehicle Applications." SAE Paper 931818. Electric Vehicles Power Systems. Warrendale, Pennsylvania: SAE, Inc., Special Publication 984, (August 1993).
4. P.F. Howard, and C.J. Greenhill. "Ballard PEM Fuel Cell Powered ZEV Bus." SAE Paper 931817. Electric Vehicle Power Systems. Warrendale, Pennsylvania: SAE Inc., Special Publication 984, pp. 113-120 (August 1993).
5. U.S. Department of Energy. Idaho National Engineering Laboratory. *USABC Electric Vehicle Battery Test Procedures Manual: Revision 1*, Report DOE/ID-10479, July 1994.
6. D.H. Swan, and A.J. Appleby. "Fuel Cells for Electric Vehicles, Knowledge Gaps and Development Priorities." Proceedings of The Urban Electric Vehicle, Stockholm, Sweden, pp 457-468 (May 1992).
7. Kenneth Wark. Thermodynamics. New York: McGraw-Hill Book Company, 1983, p. 628.